Cylindrical Antenna Theory for the Analysis of Whole-Body Averaged Specific Absorption Rate

Article *in* IEEE Transactions on Antennas and Propagation · November 2015
DOI: 10.1109/TAP.2015.2478484

CITATIONS
5

READS
64

3 authors:

Behailu Kibret
Monash University (Australia)
31 PUBLICATIONS **209** CITATIONS
SEE PROFILE

Assefa Teshome
Victoria University Melbourne
14 PUBLICATIONS **49** CITATIONS
SEE PROFILE

Daniel T. H. Lai
Victoria University Melbourne
124 PUBLICATIONS **946** CITATIONS
SEE PROFILE

[12] H. Lebret and S. Boyd, "Antenna array pattern synthesis via convex optimization," *IEEE Trans. Signal Process.*, vol. 45, no. 3, pp. 526–532, Mar. 1997.
[13] J. Córcoles, M. González, and J. Rubio, "Multiobjective optimization of real and coupled antenna array excitations via primal-dual, interior point filter method from spherical mode expansions," *IEEE Trans. Antennas Propag.*, vol. 57, no. 1, pp. 110–121, Jan. 2009.
[14] Z. Luo, W. Ma, A. So, Y. Ye, and S. Zhang, "Semidefinite relaxation of quadratic optimization problems," *IEEE Signal Process. Mag.*, vol. 27, no. 3, pp. 20–34, May 2010.
[15] B. Fuchs, "Application of convex relaxation to array synthesis problems," *IEEE Trans. Antennas Propag.*, vol. 62, no. 2, pp. 634–640, Feb. 2014.
[16] *IEEE Standard Definitions of Terms for Antennas*. IEEE Standard 145-2013, 2014.
[17] CST Computer Simulation Technology. (2014). *3D EM Field Simulation—CST Computing Simulation Technology* [Online]. Available: http://www.cst.com
[18] M. S. Andersen, J. Dahl, and L. Vandenberghe. (2013). *CVXOPT: A Python Package for Convex Optimization, Version 1.1.6* [Online]. Available: http://cvxopt.org

Cylindrical Antenna Theory for the Analysis of Whole-Body Averaged Specific Absorption Rate

Behailu Kibret, Assefa K. Teshome, and Daniel T. H. Lai

***Abstract*—International guidelines and standards on whole-body radio-frequency (RF) dosimetry use the whole-body averaged specific absorption rate (WBA-SAR) as a surrogate metric to quantify the temperature rise in the body. This study proposes the analysis of whole-body RF dosimetry for far-field exposure of a grounded human body in the frequency range of 1–150 MHz based on a semianalytic approach of cylindrical antenna theory. The human body is represented by a lossy homogeneous cylindrical monopole antenna. For the first time, an explicit model for the resonance frequency of a grounded human body is proposed. The model captures the effects of the human body weight, height, and the dielectric properties. This study also addresses the effect of shoes on WBA-SAR. It is found that the resonance frequency for the WBA-SAR with shoe effect is higher than reported from using the bare-footed models, as confirmed by theory and measurement.**

***Index Terms*—Cylindrical antenna, resonance frequency, RF dosimetry, specific absorption rate (SAR), whole-body averaged SAR (WBA-SAR).**

I. Introduction

One of the technological breakthroughs is the increasing use of electromagnetic fields for a broad spectrum of applications in day-to-day life. At the same time, the concern of the possible adverse effects of electromagnetic fields is also growing alongside in the society. Excessive whole-body exposure to the radio-frequency (RF) electromagnetic fields has the effect of increasing the human body core temperature. To address this issue, international standards [1] and guidelines [2] have been developed that use the whole-body averaged specific absorbtion rate (WBA-SAR) as a proxy metric to quantify the temperature rise in the body. WBA-SAR is the amount of RF power absorbed by the human body averaged over the whole body. Since it is not suitable to measure the WBA-SAR inside the human body, computational results are often used to relate the WBA-SAR with external measurable quantities, such as the incident electric field.

Prior RF dosimetry studies made use of simple human body models based on common geometrical shapes so that analytical solutions or simple numerical techniques could be applied [3], [4]. Currently, the most common way of computing the WBA-SAR is performed by applying the finite-difference time-domain (FDTD) technique on realistic high-resolution voxel models of the human body [5]–[7]. Through the whole-body RF dosimetry studies, the analogy between the human body and a quarter-wave monopole antenna has been widely reported. However, not much has progressed in the analysis of the computation results from the antenna theory perspective. Among the few studies that focus on antenna theory, the similarity between a quarter-wave monopole antenna and a grounded human body has been reported in [8]–[10] from statistical analyses of the FDTD computation results from applying the human body voxel models. Also, other earlier studies have employed the cylindrical antenna theory to calculate the induced current inside the human body when it is exposed to electromagnetic fields. The cylindrical antenna model of the human body was used in the analysis of the electromagnetic field exposure from power transmission lines by King *et al.* [11] based on a semi-analytic approach. For similar power-line frequency, Poljak *et al.* [12] used the method of moments (MoM) to calculate the induced current in thick-wire model of the human body. Both approaches provided reasonably accurate results compared to the results found using the FDTD algorithm on voxel-based models of the human body [13]. A two-term approximation method was utilized by King [14] for higher frequency range of 50–200 MHz to calculate induced current in the cylindrical dipole antenna model of an isolated or ungrounded human body with the objective of quantifying the amount of current induced inside the body of amateur radio operators. Within this context, we propose a semianalytic approach, based on the three-term approximation method, to analyze the WBA-SAR based on an equivalent cylindrical monopole antenna representation of a grounded human body. The cylindrical monopole antenna represents a realistic case of a person standing on the ground, whereas a cylindrical dipole antenna represents a human body in free space.

In this study, a grounded human body is represented by an equivalent cylindrical monopole antenna grounded on an infinite conductive plane as shown in Fig. 1. Early studies have used simple geometrical shapes, such as the cylinder, prolate spheroid, or cuboid, to approximate the human body [3], [4]. Unlike previous (9) studies, our study is not concerned with using the cylinder to approximate the physical attributes of the human body; rather, it is concerned with defining the parameters of a cylindrical monopole antenna that produce equivalent WBA-SAR values compared to the FDTD computations on realistic voxel models of the human body. Also, the main objective of this study is not finding alternative analytic expressions for the WBA-SAR, since the state-of-the-art in electromagnetic computations allows a much better approach. Instead, we propose semianalytic expressions that are used to analyze the whole-body RF dosimetry in a more convenient and flexible way than can be achieved using FDTD. Moreover, the proposed model integrates the mechanism of how different parameters of the human body affect the WBA-SAR. The analysis focuses on the effect of human body attributes, such as height, weight, and the dielectric properties of the tissues with additional look at the effect of shoes. The approach is valid for the frequency range lower

Manuscript received March 02, 2015; revised June 09, 2015; accepted September 07, 2015. Date of publication September 14, 2015; date of current version October 28, 2015.

The authors are with the College of Engineering and Science, Victoria University, Footscray, VIC 3030, Australia (e-mail: behailu.kibret@live.vu.edu.au).

Color versions of one or more of the figures in this communication are available online at http://ieeexplore.ieee.org.

Digital Object Identifier 10.1109/TAP.2015.2478484

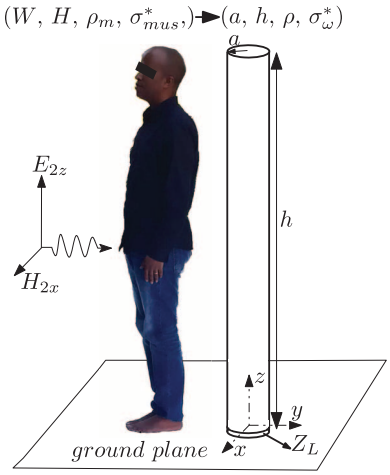

Fig. 1. Equivalent cylindrical monopole antenna representation of a grounded human body.

than 150 MHz, which is an important frequency range in whole-body RF dosimetry since it contains the resonance frequency of both the grounded and isolated human bodies. In RF dosimetry, the resonance frequency is defined as the frequency where the maximum WBA-SAR occurs. Recently, a similar approach was applied to analyze the WBA-SAR of an isolated or ungrounded human body [15], to study the antenna effects of the human body on human body communications (HBC) [16], and to characterize the antenna nature of the human body [17]. Moreover, the practical application of the equivalent antenna representation of the human body has proved to be accurate at measuring the ankle current, as reported in [18].

In this communication, first, the expression for the total induced axial current and the WBA-SAR of the equivalent cylindrical monopole antenna are provided based on the three-term approach. Next, the parameters of the equivalent cylindrical antenna are related to the physical attributes of the human body. From the FDTD calculated WBA-SAR values of three voxel models, numerical values of the parameters of the cylinders representing the adult males, adult females, and children are defined. In order to demonstrate the validity of the approach, explicit formula for the resonance frequency is proposed and validated with FDTD-based results of 11 different voxel models that represent different age groups, sex, and race. Lastly, the effects of the height, weight, and the dielectric properties of the body are discussed. More emphasis is given to the real-life notion of WBA-SAR by analyzing the effect of shoes on the WBA-SAR and the resonance frequency, which is further supported by experimental results.

II. Theory

A. Total Induced Axial Current

It was assumed that a time-harmonic vertically polarized plane wave induces a rotationally symmetric current density inside the equivalent cylindrical monopole antenna representing a grounded human body as shown in Fig. 1. The approximate analytic expression for the total induced axial current inside the equivalent cylindrical monopole antenna of height h, radius a, and complex conductivity σ^*_ω was driven based on the three-term approximation of the axial current in an imperfectly conducting and loaded receiving cylindrical antenna in [16], [19], and [20] as

$$I_{1z}(z) = V_0^e v(z) + U_0 u(z). \tag{1}$$

V_0^e and U_0 in (1) are defined as

$$V_0^e = -I_{sc}(0)\frac{2Z_A Z_L}{2Z_A + Z_L}, \quad U_0 = \frac{E_0}{k_2} \tag{2}$$

and

$$v(z) = \frac{j2\pi k_2}{\zeta_0 \gamma \Psi_{dR} \cos(\gamma h)}\left[\sin\gamma(h-|z|) + T_U(\cos\gamma z - \cos\gamma h) + T_D\left(\cos\frac{1}{2}k_2 z - \cos\frac{1}{2}k_2\ h\right)\right] \tag{3}$$

$$u(z) = \frac{j4\pi}{\zeta_0}\left[H_U(\cos\gamma z - \cos\gamma h) + H_D\left(\cos\frac{1}{2}k_2 z - \cos\frac{1}{2}k_2\ h\right)\right] \tag{4}$$

where $E_0(Vm^{-1})$ is the incident electric field at the surface of the cylinder; k_2 is the free-space wave number; $Z_A = 1/(2v(0))$ (Ω) is the driving-point impedance of the same cylinder when driven at the base; Z_L (Ω) is the load impedance at the base of the cylinder; $I_{sc}(0) = U_0 u(0)$ is the current at the base when there is no load; and ζ_0 is the free-space impedance. The expressions of the frequency-dependent coefficients Ψ_{dR}, T_U, T_D, H_U, and H_D in (3) and (4) are given in [16], which involve integrals that are solved numerically. Based on King [19], the imperfectly conducting nature of the equivalent cylindrical antenna was characterized by the complex propagation constant γ, which was defined as

$$\gamma = k_2\sqrt{1 - j\frac{4\pi z^i}{k_2\zeta_0\Psi_{dR}}} \tag{5}$$

where z^i $(\Omega \mathrm{m}^{-1})$ is the surface impedance per unit length of the cylinder that was defined in [19] as

$$z^i = \frac{\kappa}{2\pi a\sigma^*_\omega}\frac{J_0(\kappa a)}{J_1(\kappa a)} = r^i + jx^i \tag{6}$$

where J_0 and J_1 are the zeroth- and first-order Bessel functions, respectively. The term κ was also defined as

$$\kappa = \sqrt{-j\omega\mu_0\epsilon_0\left(\frac{\sigma^*_\omega}{\epsilon_0} - j\omega - \frac{4\pi z^i}{\mu_0\Psi_{dR}}\right)} \tag{7}$$

where μ_0 is the permeability of free space, ϵ_0 is the permittivity of free space, and ω is the angular frequency.

B. Total Power Dissipated Inside the Cylinder

The total average power dissipated P_{diss} inside the cylinder can be obtained as [21]

$$P_{diss} \simeq \frac{1}{2}\int_0^h r^i\,|I_{1z}(z)|^2\,dz \tag{8}$$

where r^i is the real part of z^i(6). WBA-SAR is defined as the total average RF power absorbed by the human body divided by the total mass of the body [5]. Thus, for a homogenous cylinder of height h, radius a, density ρ, and weight $W_c = \rho\pi a^2 h$, the total average absorbed power per unit mass $WSAR_{cyl}$ was defined as

$$WSAR_{cyl} = \frac{P_{diss}}{W_c} = \frac{r^i}{2\rho\pi a^2 h}\int_0^h |I_{1z}(z)|^2\,dz. \tag{9}$$

TABLE I
CONSTANTS OF PROPORTIONALITY

	Adult male	Adult female	Child
L_1	$\sqrt{5}$	$\sqrt{5}$	$\sqrt{5}$
L_2	0.25	0.21	0.16
L_3	0.38	0.44	0.60

C. Parameters of the Equivalent Cylindrical Antenna

In this study, the parameters of the equivalent cylindrical monopole antenna were defined based on the anatomical parameters of the human body. The equivalent cylindrical antenna parameters taken were its radius a (m), density ρ (kgm^{-3}), height h (m), and the complex conductivity σ_ω^* (Sm^{-1}) of the material forming the cylinder. Also, the human body anatomical parameters used were the weight W (kg), height H (m), average density ρ_m (kgm^{-3}), and the complex conductivity of muscle σ_{mus}^* (Sm^{-1}), as shown in Fig. 1. The muscle tissue was chosen due to the fact that it is one of the major tissues in the body; and also, there is widespread use of the muscle tissue in homogenous models of the human body [8].

Using similar explanations given in our previous study of an equivalent cylindrical dipole antenna for the representation of an isolated human body in [15], the parameters of the cylinder were defined as

$$a = L_1\sqrt{\frac{W}{\pi\rho_m H}} \tag{10}$$

$$h = H \tag{11}$$

$$\sigma_\omega^* = L_2\frac{2x}{3-x}\sigma_{mus}^* \tag{12}$$

$$\rho = L_3\frac{\rho_m}{x} \tag{13}$$

where L_1, L_2, and L_3 are the constants of proportionality; σ_{mus}^* was defined based on the 4-Cole–Cole dispersions [22]; $\rho_m \simeq 1050$ kgm^{-3} [23]; and x is a function of the lean-body-mass of the human subject, which was defined in [15]. The parameter x for males was defined as

$$x = 0.321 + \frac{1}{W}\left(33.92H - 29.53\right) \tag{14}$$

and for females as

$$x = 0.295 + \frac{1}{W}\left(41.81H - 43.29\right). \tag{15}$$

As shown in (14) and (15), the subject-specific parameter x is a function of the weight and height of the human subject. Thus, it was assumed that x correlates with the fat-to-muscle ratio of the human subject, which affects the value of WBA-SAR [24].

For a given frequency, height, and weight of a human subject, the expression of $WSAR_{cyl}$ in (9) simplifies to a function of three unknowns, namely L_1, L_2, and L_3. The values of these unknowns were evaluated by iteratively comparing the value of $WSAR_{cyl}$ with known FDTD computed WBA-SAR values of three voxel models representing an adult male, an adult female, and a child. For the frequency range of 1–150 MHz, $Z_L = 0$, and $E_0 = 1$ Vm^{-1} rms, the values of the unknowns that produced the least-average difference between the $WSAR_{cyl}$ and the known WBA-SAR were taken as the values of L_1, L_2, and L_3. The data for the FDTD-based WBA-SAR values were taken from the literature [5], [24]. It was found that values of the constants of proportionality depend on the sex and age of the human subjects as shown in Table I. The WBA-SAR calculated using (9) and the corresponding FDTD calculated WBA-SAR of the voxel models are shown in Fig. 2.

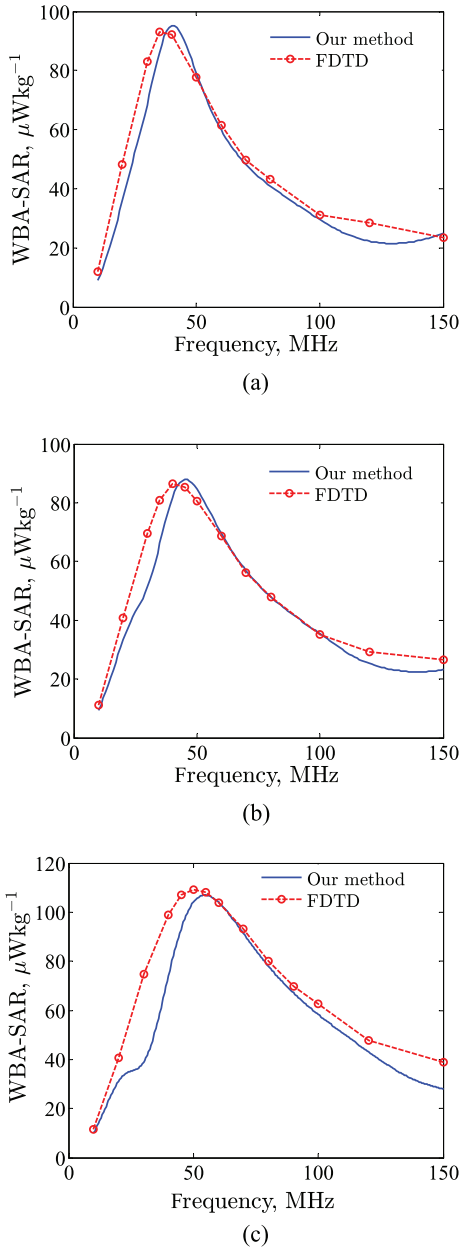

Fig. 2. Comparison of the WBA-SAR calculated using the equivalent cylindrical antenna and from FDTD on voxel models for $E_0 = 1$ Vm^{-1} rms. (a) Adult male. (b) Adult female. (c) 10-year-old child.

III. RESULTS

The values of L_1, L_2, and L_3 were derived based on the FDTD-computed results of three voxel models. Therefore, their validity to express the WBA-SAR of other human voxel models, other than those used for their derivation, has to be assessed. This was done by deriving a formula for the resonance frequency.

Assuming the load impedance at the base of the cylinder $Z_L = 0$, the total axial current can be expressed as

$$I_{1z}(z) = U_0 u(z). \tag{16}$$

Replacing $I_{1z}(z)$ in (9) with the expression in (16), the maximum value of $WSAR_{cyl}$ with respect to frequency can be found by differentiating (9) with respect to the complex propagation constant γ(5).

TABLE II
COMPARISON OF THE CALCULATED RESONANCE FREQUENCIES WITH THAT OF THE FDTD COMPUTED

Voxel model	W	H	Sex	f_{res}	FDTD f_{res}	Diff. (%)
TARO	65	1.73	m	42.09	39	–7.92
HANAKO	53	1.60	f	45.13	45	–0.29
BAFB	105	1.88	m	37.08	38	2.42
Duke	70	1.74	m	41.38	40	–3.45
Ella	58	1.6	f	44.46	42	–5.86
Billie	34	1.48	f	51.07	51	–0.14
Thelonious	17	1.17	m	64.44	66	2.36
TARO 7 yr	23	1.2	m	59.99	61	1.66
TARO 5 yr	17	1.05	m	67.29	75	10.28
TARO 3 yr	13	0.90	m	75.83	83	9.46
Pregnant	58	1.61	f	44.34	46	3.61

The weight W is in kg, the height H in m, the resonance frequencies in MHz. Diff. is the percentage difference.

It was found that the maximum occurs when

$$\gamma h = k_2 \left(\sqrt{1 - \left| \frac{j4\pi z^i}{k_2 \zeta_0 \Psi_{dR}} \right|} \right) h \simeq 1. \tag{17}$$

Since k_2 and h are real valued, the imaginary part of the complex term in the bracket is negligible; thus, the second term in the square root was approximated with its magnitude. The expression in (17) can be written in quadratic form by replacing z^i with its expression in (6) as

$$k_2^2 - \left| \frac{j2}{\zeta_0 \Psi_{dR}} \frac{\kappa}{\sigma_\omega^*} \frac{J_0(\kappa a)}{J_1(\kappa a)} \right| \frac{k_2}{a} - \frac{1}{h^2} \simeq 0. \tag{18}$$

For the radius a and complex conductivity σ_ω^* of the three human body models used, when the expression in the absolute value in (18) is computed for the frequency range of interest, the result tends to approach the constant value of 0.12. The frequency-dependent parameters inside the absolute value are functions of the complex conductivity of muscle, which has approximately constant magnitude in the frequency range of interest. Also, for the values of the radius a used, the values of the Bessel functions change slightly. Therefore, replacing this term with its equivalent computed value 0.12, using the relation $k_2 = \omega\sqrt{\epsilon_0 \mu_0} = \omega/c = 2\pi f_{res}/c$, and replacing the radius a with (10), the quadratic equation can be solved for the resonance frequency f_{res} as

$$f_{res} \simeq \frac{c}{4\pi} \left[1.742 \left(\frac{\pi H}{W} \right)^{\frac{1}{2}} + \left(3.0345 \frac{\pi H}{W} + \frac{4}{H^2} \right)^{\frac{1}{2}} \right] \tag{19}$$

where c is the speed of light in free space.

The comparison of the resonance frequencies calculated using (19) to the FDTD-based resonance frequencies of 11 voxel models that were developed by different authors and reported in [8] is shown in Table II. The formulation of the resonance frequency proposed in (19) estimates the FDTD results of the 11 voxel models with an average percentage difference of 4.31% as shown in the last column of the table.

IV. DISCUSSION

The semianalytic approach followed here to analyze the equivalent cylindrical antenna and to calculate the total axial current has been proved to be accurate in cylindrical antenna analysis [25], providing

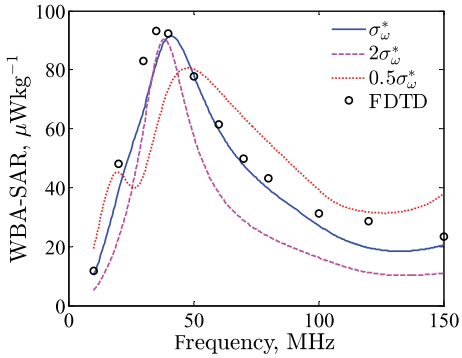

Fig. 3. Comparison of the WBA-SAR calculated for different values of the complex conductivity.

that the condition $k_2 a \ll 1$ and $h \gg a$ is satisfied. For the equivalent cylindrical antennas used in this communication, the condition can be satisfied for the frequency range lower than 150 MHz, which is an important frequency range in the whole-body RF dosimetry as it contains the resonance frequency.

The formulation proposed in (19) is based on the three voxel models representing an adult male, adult female, and a 10-year-old child; therefore, it became less accurate for very young children when comparing the predicted resonance frequency. For example, the percentage difference between the FDTD resonance frequency and the estimated resonance frequency for the 5- and 3-year-old version of TARO is about 10%, which is much larger compared to the other models.

A. Effect of the Height and Weight

From the expression of the resonance frequency in (19), it can be seen that the resonance frequency depends on the weight and the height. The weight parameter in the formulation of the resonance frequency determines the radius of the cylindrical antennas or it represents how "wide" a person is. For example, as shown in Table II, the model Thelonious and TARO 5 years have equal weight of 11 kg and height of 1.17 and 1.05 m, respectively. Their resonance frequencies are 64.44 and 67.29 MHz, respectively. This shows that a tall person has lower resonance frequency compared to a shorter person of the same weight. Similarly, from (19), it can be seen that a heavier person has a lower resonance frequency compared to a lighter person of the same height. For example, this can be seen by comparing two subjects of weight 30 and 40 kg and equal height of 1.4 m. Their corresponding resonance frequencies are 53.52 to 50.54 MHz, respectively.

B. Effect of the Dielectric Properties of Tissues

In order to observe the effect of the dielectric property on the WBA-SAR, the complex conductivity of the equivalent cylindrical antenna representing the adult male was doubled and halved. The predicted WBA-SAR is shown in Fig. 3. It can be seen that when the conductivity was doubled, the frequency characteristics of the WBA-SAR became narrower. This is expected from the perspective of antenna theory. It is well known that a thin and highly conductive wire antenna has a narrowband frequency response, whereas a thick and imperfectly conducting cylindrical antenna has broadband response [26]. Also, when the conductivity was halved, the WBA-SAR got broader. This effect was also observed when comparing the WBA-SAR of the adult male and the adult female as shown in Fig. 2. The WBA-SAR of the female model is slightly broader than that of the male, which could be due

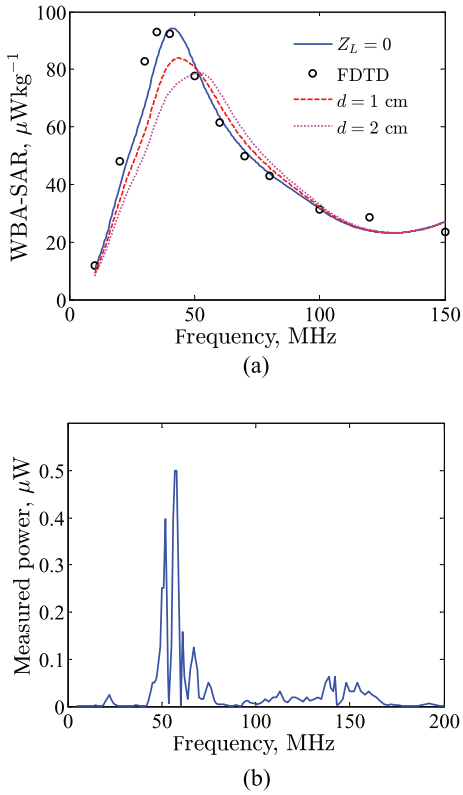

Fig. 4. (a) Effect of load due to inserting rubber of thickness d 1 and 2 cm at the base of the equivalent cylindrical antenna representing NORMAN. (b) Measured power when a subject is illuminated by electromagnetic field.

to the smaller muscle mass percentage or higher fat in females. The conductivity of muscle is larger than fat.

C. Effect of Shoes on Whole-Body RF Dosimetry

Most studies on WBA-SAR were based on voxel models of a bare-footed human body. The effect of shoes on the WBA-SAR and the resonance frequency was reported in [6], but a detailed analysis was not given. All the preceding calculations were performed based on the assumption that the equivalent cylindrical monopole antenna is grounded on a perfectly conducting plane; in other words, the load impedance was set to zero, $Z_L = 0$. But, in real life, people wear shoes; therefore, it is more relevant to see how a load at the base of the cylinder affects the WBA-SAR and the resonance frequency. Using the equivalent cylindrical antenna representation of the adult male, the load impedance of rubber ($\epsilon_r = 3.5$) with thickness of 1 and 2 cm is inserted at the base of the cylinder. Load insertion at the base has the effect of decreasing the value of WBA-SAR and shifting the resonance frequency to a higher band. For example, the insertion of 2-cm rubber at the base of the cylinder decreased the WBA-SAR by 16 μWkg^{-1} (for $E_0 = 1$ Vm^{-1} rms) shifting the resonance frequency from 40 to 53 MHz as shown in Fig. 4(a). This prediction was supported by measurements carried out in our previous study on the antenna effects of the human body [16]. As described in our previous study, a human subject, who wore a pair of rubber-soled shoes and has an equivalent anatomical parameters with NORMAN, was illuminated with electromagnetic field generated from a monopole antenna located 3 meters away. It was found that the measured power due to the electric current established when the subject touches an electrode attached to a spectrum analyzer has resonance near 55 MHz as shown in Fig. 4(b). This suggests that the WBA-SAR resonance frequency in a real scenario might be larger than the predicted value from using bare-footed voxel models. Our calculation and measurement suggest that, for an average size adult human with shoes on, the resonance frequency is between 50 and 60 MHz compared to the 35 to 45 MHz predicted for bare-footed voxel models.

Similarly, assuming that the load impedance is due to a gap (air) between the cylinder base and the ground, our calculation showed that a separation of 5 cm shifts the resonance frequency of the adult male to 65 MHz, which is equivalent to the resonance frequency of the isolated adult male. Also, a 1-cm cylinder base-to-ground separation shifts the resonance frequency to 56 MHz.

The proposed formulations can be used in the analysis of the WBA-SAR in the frequency range of 1–150 MHz, which contains the FM band. Moreover, the formulation of the resonance frequency and the analysis of the effect of shoes on the induced current have applications in the investigation of the electromagnetic phenomenon in HBC and in the survey of the possible application of the human body as antenna for implant wireless communications. For example, it has been explained how the minimum channel attenuation in HBC aligns with the resonance frequency of the induced currents in the human body exposed to electromagnetic fields [16]. In order to investigate the possible application of using the human body as an antenna for implant wireless communications, the formulation of the resonance frequency can also be useful to estimate the frequency at which maximum RF power radiates out of the body.

V. Conclusion

The whole-body RF dosimetry was analyzed based on the equivalent cylindrical antenna representation of the human body of normal BMI in the frequency range lower than 150 MHz. The equivalent cylindrical antenna representation of the human body is parameterized as adult males, adult females, and children based on the FDTD computation results of three realistic voxel models. Explicit formula for the resonance frequency was proposed, which was used to validate the proposed cylindrical antenna model. The effects of the height, the weight, and the dielectric properties of the body are discussed. More importantly, the proposed equivalent cylindrical antenna suggests that the real-body resonance frequency could be higher than previous theoretical frequencies based on bare-footed voxel models. The proposed approach can be applied to study the electromagnetics in HBC, which has operation frequency less than 150 MHz.

References

[1] *IEEE standard for safety levels with respect to human exposure to radio frequency electromagnetic fields, 3 kHz to 300 GHz*, IEEE Standard C95-1, 2005.

[2] ICNIRP (International Commission on Non-Ionising Radiation Protection), "Guidelines for limiting exposure to time-varying electric, magnetic, and electromagnetic fields (up to 300 GHz)," *Health Phys.*, vol. 74, no. 4, pp. 494–522, 1998.

[3] C. H. Durney, "Electromagnetic dosimetry for models of humans and animals: A review of theoretical and numerical techniques," *Proc. IEEE*, vol. 68, no. 1, pp. 33–40, Jan. 1980.

[4] O. P. Ghandi, "State of the knowledge for electromagnetic absorbed dose in man and animals," *Proc. IEEE*, vol. 68, no. 1, pp. 24–32, Jan. 1980.

[5] P. J. Dimbylow, "FDTD calculations of the whole-body average SAR in an anatomically realistic voxel model of the human body from 1 MHz to 1 GHz," *Phys. Med. Biol.*, vol. 42, no. 3, pp. 479–490, 1997.

[6] P. J. Dimbylow, "Fine resolution calculations of SAR in the human body for frequencies up to 3 GHz," *Phys. Med. Biol.*, vol. 47, no. 16, pp. 2835–2846, 2002.

[7] J. Wang, O. Fujiwara, S. Kodera, and S. Watanabe, "FDTD calculation of whole-body average SAR in adult and child models for frequencies from 30 MHz to 3 GHz," *Phys. Med. Biol.*, vol. 51, no. 17, pp. 4119–4127, 2006.
[8] A.Hirata *et al.*, "Estimation of the whole-body averaged SAR of grounded human models for plane wave exposure at respective resonance frequencies," *Phys. Med. Biol.*, vol. 57, no. 24, p. 8427, 2012.
[9] A. Hirata, O. Fujiwara, T. Nagaoka, and S. Watanabe, "Estimation of whole-body average SAR in human models due to plane-wave exposure at resonance frequency," *IEEE Trans. Electromagn. Compat.*, vol. 52, no. 1, pp. 41–48, Feb. 2010.
[10] K. Yanase and A. Hirata, "Effective resistance of grounded humans for whole-body averaged SAR estimation at resonance frequencies," *Prog. Electromagn. Res. B*, vol. 35, pp. 15–27, 2011.
[11] R. W. P. King and S. S. Sandler, "Electric fields and currents induced in organs of the human body when exposed to ELF and VLF electromagnetic fields," *Radio Sci.*, vol. 31, no. 5, pp. 1153–1167, 1996.
[12] D. Poljak and V. Roje, "Currents induced in human body exposed to the power line electromagnetic field," in *Proc. 20th Annu. Conf. IEEE Eng. Med. Biol. Soc.*, 1998, vol. 6, pp. 3281–3284.
[13] O. P. Ghandi and J. Chen, "Numerical dosimetry at power-line frequencies using anatomically based models," *Bioelectromagn. Suppl.*, vol. 13, no. S1, pp. 43–60, 1992.
[14] R. W. P. King, "Electric current and electric field induced in the human body when exposed to an incident electric field near the resonant frequency," *IEEE Trans. Microw. Theory Techn.*, vol. 48, no. 9, pp. 1537–1543, Sep. 2000.
[15] B. Kibret, A. K. Teshome, and D. T. H. Lai, "Analysis of the whole-body averaged specific absorption rate (SAR) for far-field exposure of an isolated human body using cylindrical antenna theory," *Prog. Electromagn. Res. M*, vol. 38, pp. 103–112, 2014.
[16] B. Kibret, A. K. Teshome, and D. T. H. Lai, "Human body as antenna and its effect on human body communications," *Prog. Electromagn. Res.*, vol. 148, pp. 193–207, 2014.
[17] B. Kibret, A. K. Teshome, and D. T. H. Lai, "Characterizing the human body as a monopole antenna," *IEEE Trans. Antennas Propag.*, vol. 63, no. 10, pp. 4384–5392, 2015.
[18] E. Aslan and O. P. Gandhi, "Human-equivalent antenna for electromagnetic fields," U.S. Patent 5 394 164, Feb. 28, 1995.
[19] R. W. P. King and T. T. Wu, "The imperfectly conducting cylindrical transmitting antenna," *IEEE Trans. Antennas Propag.*, vol. 14, no. 5, pp. 524–534, Sep. 1966.
[20] C. D. Taylor, W. H. Charles, and A. A. Eugene, "Resistive receiving and scattering antenna," *IEEE Trans. Antennas Propag.*, vol. 15, no. 3, pp. 371–376, May 1967.
[21] R. W. P. King and T. T. Wu, "The imperfectly conducting cylindrical transmitting antenna: Numerical results," *IEEE Trans. Antennas Propag.*, vol. AP-14, no. 5, pp. 535–542, Sep. 1966.
[22] S. Gabriel, R. Lau, and C. Gabriel, "The dielectric properties of biological tissues: III. Parametric models for the dielectric spectrum of tissues," *Phys. Med. Biol.*, vol. 41, no. 11, pp. 2271–2293, 1996.
[23] H. J. Krzywicki and K. S. Chinn, "Human body density and fat of an adult male population as measured by water displacement," *Amer. J. Clin. Nutr.*, vol. 20, no. 4, pp. 305–310, 1967.
[24] P. Dimbylow, "Resonance behaviour of whole-body averaged specific energy absorption rate (SAR) in the female voxel model, NAOMI," *Phys. Med. Biol.*, vol. 50, no. 17, p. 4053, 2005.
[25] R. W. P. King, "The linear antenna eighty years of prograss," *Proc. IEEE*, vol. 55, no. 1, pp. 2–16, Jan. 1967.
[26] C. A. Balanis, *Antenna Theory: Analysis and Design*. Hoboken, NJ, USA: Wiley, 2005.

Modification of Sinuous Antenna Arms for UWB Radar Applications

Y. Kang, K. Kim, and W. R. Scott, Jr.

***Abstract*—The sinuous antenna is modified to improve its performance for ultrawideband (UWB) radar applications. The radiated waveforms in the time domain of typical sinuous antennas contain a long ringing tail after the chirp-like main pulse when excited by a temporally short pulse. The ringing is due to resonances that are set up on the antenna arms and are essentially eliminated by modifying the shape of the arms. The first modification removes the sharp ends where the arms terminate, and the second changes the shape of the arms where they bend. These modifications are also shown to improve the gain flatness of the antennas. Three representative sinuous antennas are fabricated, tested, and demonstrated in a monostatic radar experiment. The measured results clearly show the advantages of the improved antenna.**

***Index Terms*—Broadband antennas, log periodic antennas, radar measurements, sinuous antenna.**

I. Introduction

Since DuHamel first presented the sinuous antenna in 1987, it has been widely used by many ultrawideband (UWB) antenna designers [1]–[6]. Sinuous antennas are suitable for UWB applications and have advantages over other UWB antennas, such as resistive dipoles and Vivaldi antennas. Resistive dipoles suffer from poor radiation efficiency, and Vivaldi antennas do not have dual polarization capability, unless they are made in a 3-D structure. On the other hand, the sinuous antennas have good radiation efficiency and dual polarization capability in a 2-D structure. However, conventional sinuous antennas (CSAs) when excited by a temporally short pulse have long ringing tail. The late-time ringing of the radiated pulse clutters the image of the target in the close range. Thus, the elimination of the late-time ringing is important in closed-range target imaging applications, such as the ground-penetrating radar. Recently, in the literature, the sharp ends of the arms have often been removed to alleviate the problem [7]–[10]. It is empirically understood that the technique removes the ringing tail while keeping other advantages, such as the flat gain and impedance. To the authors' knowledge, a detailed analysis including a comparison between sinuous antennas with and without sharp ends has never been elaborated in the literature.

The first part of this communication analyzes sinuous antennas with and without sharp ends, and it is shown that the standing wave of current in the sharp ends of the sinuous arms causes the ringing tail. The detailed analysis shows that the ringing tail is reduced significantly by removing the sharp ends, and thus, the gain flatness is improved. However, the radiated waveform still contains ringing at frequencies whose values are logarithmically scaled by the inverse of the growth ratio. The gain of the antenna also shows spikes at these frequencies.

Manuscript received May 08, 2015; accepted August 29, 2015. Date of publication September 10, 2015; date of current version October 28, 2015. This work was supported by the National Research Foundation of Korea under Grant NRF-2013M1A3A3A02042444.

Y. Kang and K. Kim are with the Gwangju Institute of Science and Technology, Gwangju 500-712, South Korea (e-mail: mkkim@gist.ac.kr).

W. R. Scott, Jr., is with the School of Electrical and Computer Engineering, Georgia Institute of Technology, Atlanta, GA 30332-0250 USA (e-mail: waymond.scott@ece.gatech.edu).

Color versions of one or more of the figures in this communication are available online at http://ieeexplore.ieee.org.

Digital Object Identifier 10.1109/TAP.2015.2477492